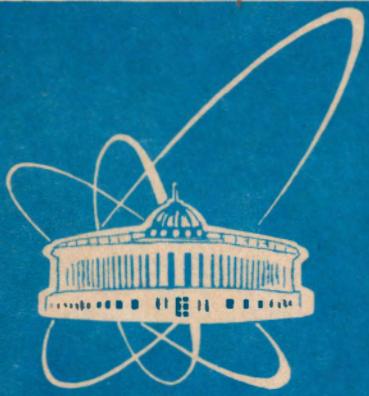

объединенный
институт
ядерных
исследований
дубна

E2-94-424

T.Gabriel[1], G.Maino[2], S.G.Mashnik

# ANALYSIS OF INTERMEDIATE ENERGY PHOTONUCLEAR REACTIONS

Talk presented at the XII International Seminar
on High Energy Physics Problems
«Relativistic Nuclear Physics and Quantum Chromodynamics»,
Dubna, Russia, 12—17 September, 1994

[1]Oak Ridge National Laboratory, Oak Ridge, Tennessee 37831, USA
[2]ENEA, Applied Physics Department, 40138 Bologna, Italy

1994

Габриел Т., Маино Дж., Машник С.Г. E2-94-424
Анализ фотоядерных реакций при промежуточных энергиях

Каскадно-экситонная модель (КЭМ) ядерных реакций развита для описания фотоядерных реакций при промежуточных энергиях. Используя КЭМ и Ок-Риджскую версию модели внутриядерного каскада при энергиях выше гигантского дипольного резонанса (ГДР) и подход групп на основе модели взаимодействующих бозонов в области ГДР, проанализированы разнообразные характеристики реакций взаимодействия фотонов с энергией до ~1,2 ГэВ с ядрами от $^{12}$C до $^{243}$Am. Обсуждается вклад различных механизмов поглощения фотонов ядрами и относительная роль различных механизмов образования частиц в этих реакциях.

Работа выполнена в Лаборатории теоретической физики им. Н.Н.Боголюбова ОИЯИ.

Препринт Объединенного института ядерных исследований. Дубна, 1994

Gabriel T., Maino G., Mashnik S.G. E2-94-424
Analysis of Intermediate Energy Photonuclear Reactions

The Cascade-Exciton Model (CEM) of nuclear reactions has been extended to describe photonuclear desintegration at intermediate energies. Using the CEM and the ORNL version of the Intranuclear Cascade Model for incident energies higher than the giant dipole resonance (GDR) region, and a group theory formalism based on the Interacting Boson Model in the GDR region, we have analyzed a variety of data for reactions induced by photons with energies up to ~1.2 GeV and target-nuclei from $^{12}$C to $^{243}$Am. The contributions of different photon absorption mechanisms and the relative role of different particle production mechanisms in these reactions are discussed.

The investigation has been performed at the Bogoliubov Laboratory of Theoretical Physics, JINR.

Preprint of the Joint Institute for Nuclear Research. Dubna, 1994

## 1. Introduction

Photonuclear reactions at intermediate energies is an useful tool for investigation such interesting problems as: short-range correlations and meson exchange currents in finite nuclei[1]; excitation of $P_{33}(1232)$, $D_{13}(1520)$, $F_{15}(1680)$, and other barion resonances[2]; study of the behaviour of pions in the *dense portion* of nuclear medium: since nuclear matter is very transparent to photons, pion photoproduction would occur, in principle, with equal probability in the whole nuclear volume, with the nucleons acting as *pion radiators*[3].

The advent of such high-duty tagged photon beam facilities as those at Mainz, Lund, Frascati, Yerevan, Bonn, and Sacley has increased the interest in photonuclear reactions and many interesting results have been recently obtained in this field. Nevertheless, an unambiguous interpretation of the observed phenomena has not been found yet[4]. So, there is not a common point of view in literature on the question about the relative role of different photon absorption mechanisms[4]: For instance, in Ref.[5] the $\Delta$ excitation plays a dominant role around $E_\gamma = 300$ MeV, while in Ref.[6] the authors conclude that the $\Delta$ is not necessary in order to explain the general future. Although all experimental analyses around and below pion production threshold show the dominance of np pairs to pp pairs coming from $\gamma$-absorption, there is still no agreement over the amount of the ratio of np to pp pairs[4]: while in Refs.[1, 7] the ratio N(pp)/N(np) grows as a function of energy in the range $E_\gamma = 100 - 400$ MeV, the work of Ref.[8] finds this ratio practically constant and about 1/10.

The law of energy and momentum conservation forbids the absorption of a photon by a free nucleon. In principle, a photon may be absorbed by an off-mass-shell, intranuclear nucleon. Recent high resolution measurements of ($\gamma$,p) reactions (see, e.g.,[9] and references therein) shown evidence of the direct knockout of protons via $\gamma p \rightarrow p$ processes; and some theoretical attempts have been done to calculate the whole proton spectra from these reactions taking into account only the one-nucleon knockout picture (see, e.g., [10, 11]).

On the other hand, some measurements on light nuclei indicate clear evidence for importance of photon absorption on three-body[12] and four-body[13] clusters, and several theoretical investigations of interaction of photons with clusters heavier than NN pairs have been also performed (see[14] and references in Ref.[13]). However, the questions about the percentage of different photodisintegration mechanisms and how does the relative contribution of 1N, 2N, 3N 4N, etc. absorption depend on photon energy and nucleus target are still open, especially for medium and heavy nuclei.

Last, we would like to remind that photonuclear reactions was an permanent subject of discussion at practically all eleven previous Dubna International Seminars on High Energy Physics Problems mainly in connection with the interesting problem of mechanisms of cumulative particle photoproduction.

The aim of our work is to analyze intermediate energy photonuclear reactions using the CEM[15] and the Oak Ridge National Laboratory version of the Intranuclear Cascade Model (ORNL ICM)[16] for incident energies higher than the GDR region, and a group theory formalism[17] based on the Interacting Boson Model (IBM)[18, 19] in the GDR region, in the hope to learn more about photodisintegration mechanisms.

## 2. Basic Assumptions of the CEM

A detailed description of the CEM may be found in Ref.[15], therefore, only its basic assumptions will be outlined here. The CEM assumes that the reactions occur in three stages. The first stage is the intranuclear cascade (IC) in which primary particles can be

rescattered several times prior to absorption by, or escape from the nucleus. The excited residual nucleus remaining after the emission of the cascade particles determines the particle-hole configuration that is the starting point for the second, preequilibrium (PREQ) stage of the reaction. The subsequent relaxation of the nuclear excitation is treated in terms of the exciton model of preequilibrium decay which includes the description of the equilibrium evaporative (EQ) third stage of the reaction. We include the emission of n, p, d, t, $^3$He and $^4$He at both the preequilibrium and the evaporative stages of reaction.

In a general case, the three components may contribute to any experimentally measured quantity. In particular, for the inclusive particle spectrum to be discussed later, we have

$$\sigma(\mathrm{p})d\mathrm{p} = \sigma_{in}[N^{cas}(\mathrm{p}) + N^{prq}(\mathrm{p}) + N^{eq}(\mathrm{p})]d\mathrm{p}.$$

The inelastic cross section $\sigma_{in}$ is not taken from the experimental data or independent optical model calculations, but it is calculated within the cascade model itself.

The cascade stage of the interaction is described by the Dubna version of the intranuclear cascade model[20]. All the cascade calculations are carried out in a three-dimensional geometry. The nuclear matter density is described by a Fermi distribution with the two parameters taken from the analysis of electron-nucleus scattering data. The energy spectrum of nuclear nucleons is estimated in the perfect Fermi gas approximation with the local Fermi energy. For characteristics of the hadron-nucleon interactions we employ the approximations given in Ref.[20].

The CEM was proposed initially to describe nucleon-induced reactions at bombarding energies below or at $\sim$ 100 MeV and developed after that for a larger interval of incident nucleon and pion bombarding energies (see, e.g., Ref.[21] and references given therein) and for the description of stopped negative pion absorption by nuclei[22]. Recently the CEM was developed[23] by including the competition between particle emission and fission at the evaporative stages of reactions and a more realistic nuclear level density (with $Z$, $N$, and $E^*$ dependences of level density parameter). Without any free parameters the CEM is able to reproduce correctly shapes and absolute values of a large variety of nucleon- and pion-induced reactions data. The recent *International Code and Model Intercomparison for Intermediate Energy Reactions*[24] showed that the CEM adequately describes nuclear reactions at intermediate energies and has one of the best predictive powers as compared to other available modern models. But, by now, the CEM was not applied to analyze photonuclear reactions.

Here we extend the CEM for description of photonuclear reactions using for the initial interaction of a photon with a nucleus the Cascade Model for Photonuclear Reaction[25] in a manner realized in Ref.[26]. We restrict ourselves to incident photon energies higher than the GDR region, and following[25] take into account processes of pion photoproduction and absorption of photons on quasideuterons pairs inside the target. The relative probabilities of these processes and the mean free path of a photon within a nucleus are determined by the corresponding cross sections. One assumes that the cross sections of interaction of photons with intranuclear nucleons are equal to the corresponding experimental cross sections of elementary free $\gamma$N interactions (for details, see[20, 25]). One determines from the experimental data also the relative probabilities of the modes

$$\gamma + p \rightarrow p + \pi^0 \quad (1)$$
$$\rightarrow n + \pi^+ \quad (2)$$
$$\rightarrow p + \pi^+ + \pi^- \quad (3)$$
$$\rightarrow p + \pi^0 + \pi^0 \quad (4)$$
$$\rightarrow n + \pi^+ + \pi^0. \quad (5)$$



Cross sections for $\gamma$n interactions are obtained by the assumption of charge symmetry. Production of three and more pions are not taken into account, that restricts the applicability of the model to photon energies of the order or less than 1.2 GeV (for details, see[20, 25]).

The cross section for the absorption of a photon by a quasideuteron pair within a nucleus is determined using the well known Levinger's formula[27]

$$\sigma_{\gamma A} = L\frac{Z(A-Z)}{A}\sigma_{\gamma d}\ , \quad (6)$$

where $A$ and $Z$ are mass and charge numbers of the target, $\sigma_{\gamma d}$ is the photodeuteron cross section, and $L$ is the quasideuteron constant. Following[25], we use in the CEM a constant value for the Levinger's constant, namely, $L = 10$.

Thus, in the approach[25] used here, the interaction of a photon with intranuclear nucleons results in production of two or three fast cascade particles inside the target. Depending on their direction and the point where photon have interacted, these cascade nucleons/pions may escape from the nucleus either without further interactions or undergoing one or several collisions with intranuclear nucleons. This stage is similar to ordinary nuclear reaction when an intermediate energy nucleon/pion incident on nucleus initiate intranuclear cascade in it. Therefore we describe the further behaviour of the reaction in the framework of the CEM, using the same fixed parameters as in Ref.[15].

## 3. Comparison between the CEM and ORNL ICM

We use here for analysis of photonuclear reactions at energies higher than the GDR region also the ORNL ICM described in details in Ref.[16], therefore only a brief discussion of this model is presented below. The ORNL ICM uses the Monte Carlo methods and assumes that the reactions occur in two stages: (1) the intranuclear cascade treated with the model of Bertini[28], and (2) the equilibrium evaporative stage described by Dresner's model[29]. The ORNL ICM takes into account pion photoproduction on nuclear nucleons and absorption of photons on quasideuteron pairs (6). But as distinct from the CEM, in the ORNL ICM only single-pion production, i.e., processes (1,2) and the corresponding ones for $\gamma$n interactions are considered. This restricts the range of photon energies to a maximum value of the order of or less 400 MeV. Sometimes, in the ORNL ICM, the Levinger's constant $L$ is considered as a free parameter and its value is chosen from the best agreement with the analyzed experimental data.

Table 1 summarizes a brief comparison between the main features of the CEM and ORNL ICM. One can see that the CEM and ORNL ICM have many common features, but differ in treatment of some essential details of reactions. Therefore, one may expect significant difference for predictions of photodisintegration characteristics calculated with these models. It is interesting to compare the results of the CEM with those of the ORNL ICM. As an example, Fig. 1 shows a comparison of calculated with the CEM and ORNL ICM total photoabsorption cross section for copper with the available experimental data[2, 30, 31]. As one can see, the predictions of both our models agree with each other and with the recent measurements[2, 30]. Some disagreement in the photon energy range 400 MeV $\leq E_\gamma \leq$ 600 MeV with the old data of Ref.[31] may be observed, but the authors of this measurement have pointed out themselves that their results disagree with other available data at these photon energies and further measurements are required. The ORNL ICM underestimates the data at $E_\gamma \geq$ 400 MeV due to not taking into account processes of production of two and more pions. The CEM also underestimates at a level of $\sim$30% the total photoabsorption cross sections at photon energies $E_\gamma \simeq 400 - 600$ MeV. This

fact may be related with an insufficient accuracy of the description of two-pion production processes (3-5) in the CEM.

**Table 1.** Comparison between the main assumptions of the CEM and ORNL ICM

| | CEM | ORNL ICM |
|---|---|---|
| Method | IC + PREQ + EQ | IC + EQ |
| IC stage | Dubna ICM[20] | Bertini's ICM[28] |
| Nuclear density distribution | $\rho(r) = \rho_0/\{exp[(r-c)/Z_1]+1\}$<br>$c = 1.07A^{1/3}$ fm, $Z_1 = 0.545$ fm<br>$\rho_n(r)/\rho_p(r) = N/Z$<br>$\rho(r) = \alpha_i\rho(0); i = 1,...,7$<br>$\alpha_1 = 0.95$, $\alpha_2 = 0.8$, $\alpha_3 = 0.5$,<br>$\alpha_4 = 0.2$, $\alpha_5 = 0.1$, $\alpha_6 = 0.05$,<br>$\alpha_7 = 0.01$ | the same<br>the same<br>the same<br>$\rho(r) = \alpha_i\rho(0); i = 1,...,3$<br>$\alpha_1 = 0.9$, $\alpha_2 = 0.2$,<br>$\alpha_3 = 0.01$ |
| Pion potential | $V_\pi = 25$ MeV | $V_\pi = V_N$ |
| Mean binding nucleon energy | $B_N \simeq 7$ MeV | the same |
| $\gamma A$: photo-absorption (QDM) | $\sigma_{\gamma A} = L(NZ/A)\sigma_{\gamma d}$<br>$L = 10$<br>40 MeV $\leq E_\gamma \leq$ 1.2 GeV | the same<br>$7.1 \leq L \leq 12.5$<br>40 MeV $\leq E_\gamma \leq$ 400 MeV |
| $\gamma A$: pion production | processes (1,2)<br>processes (3-5) | the same<br>are absent |
| Condition for passing from the IC stage | $\mathcal{P} = \lvert (W_{mod.} - W_{exp.})/W_{exp.} \rvert$,<br>$\mathcal{P} = 0.3$, see[15] | cutoff energy $\sim 7$ MeV |
| PREQ stage | under[15] | is absent |
| EQ stage | n, p, d, t, $^3$He, $^4$He emission + fission [23] | n, p, d, t, $^3$He, $^4$He emission[29] |
| Level density | $a = a(Z, N, E^*)$ [23] | $a = const \times A$ |
| Fission | under[23] | is absent |

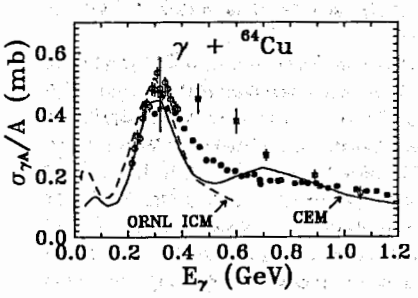


**Fig. 1.** Total photonuclear absorption cross section per nucleon plotted as a function of photon energy for $^{64}$Cu. The full and dashed lines show the results obtained with the CEM and ORNL ICM, respectively. Experimental points are from: [30] (o), [31] (□), and [2] (•, obtained from an averaging of the data for Li, C, Al, Cu, Sn, and Pb).

In the upper part of Fig. 2 are displayed the mean multiplicities of n, p, $\pi^-$, and $\pi^+$ photoproduction on copper calculated with the CEM and ORNL ICM as equal to total photoabsorption cross sections divided by the corresponding particle production yields. One can see that although our models differ in several important features, they predict quit closed results for nucleon and pion multiplicities.

To illustrate the relative role of different proton production mechanisms, as an example, the cascade, preequilibrium, and the evaporative components of proton multiplicity predicted by the CEM are shown separately in the lower part of Fig. 2.



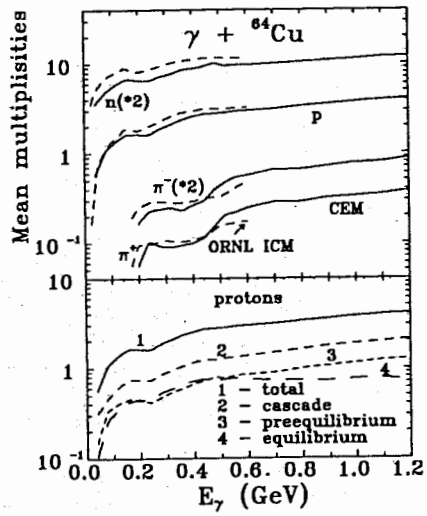


**Fig. 2.** Mean multiplicities of n, p, $\pi^-$, and $\pi^+$ photoproduction on $^{64}$Cu (upper graph) predicted by the CEM (full lines) and ORNL ICM (dashed lines). On the lower graph, the full line show the total mean multiplicity of protons calculated with the CEM, and the dashed lines 2, 3, and 4 show the contribution of the cascade, preequilibrium, and the evaporative components, respectively.

One can see that in the whole photon energy range regarded here the main contribution to proton multiplicity comes from emission at the cascade stage of reaction. For this, $^{64}$Cu target, the preequilibrium and evaporative components are of the same order of magnitude, about twice lower than the cascade component, and the relative contribution of proton emission at the compound stage of reaction decreases slowly with increasing photon energy in the region $E_\gamma \geq 500$ MeV.

## 4. Exemplary Results and Discussion

**4.1. Energy Region Above the GDR.** We analyzed using the CEM and ORNL ICM a variety of data for reactions induced by bremsstrahlung and tagged photons. For the sake of brevity we present here only some exemplary results. As an example, in Fig. 3

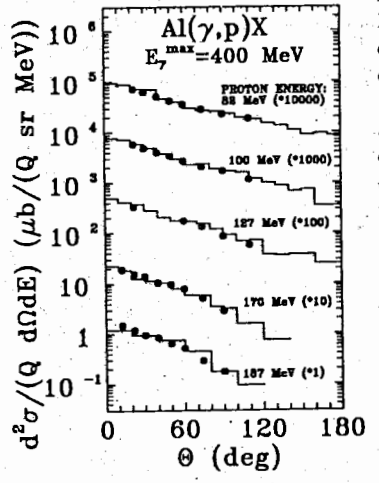


**Fig. 3.** Photoproton angular distribution for 400-MeV bremsstrahlung on Al. The histograms are calculated with the ORNL ICM[16]; experimental data are from Ref.[32].

a comparison is made between the prediction of the ORNL ICM and experimental data[32] consisting of photoproton angular distribution for 400-MeV bremsstrahlung incident on Al. These spectra have been calculated using for the Levinger's constant the value $L = 7.1$[16]. Similar results have been obtained for other targets, photon incident energies, and charged pion spectra.

The individual contributors to the total proton angular distribution, i.e., those protons produced when the initial photon is absorbed by a quasideuteron and those protons produced when the initial photon produces a pion, at a proton energy of 82 MeV, are shown in Fig. 4. It is quite apparent that the shape of the spectra could not be predicted without an excellent balance between the initial interactions[16].

We have calculated using our models also total cross sections for production of different residual nuclei resulting from bremsstrahlung and monoenergetic photons on several nuclei, and obtained an overall satisfactorily agreement between the calculated and experimental values (see, e.g., Ref.[16]).

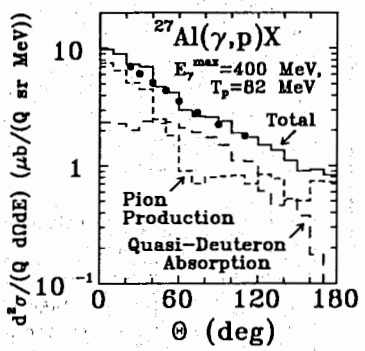


**Fig. 4.** Quasideuteron and pion-production contributions to the total photoproduction angular distribution at 82 MeV proton energy for 400-MeV bremsstrahlung on Al[16].

Using the well known Weisskopf statistical theory of particle emission from excited compound nuclei and the Bohr and Wheeler theory of fission realized in the CEM as described in Ref.[23] we analyzed a variety of data on nuclear fissilities and photofission cross sections at photon energies 40 MeV $\leq E_\gamma \leq$ 1.2 GeV. We have found out that for every target it is possible to select a model for fission barrier $B_f$, level density parameter $a(Z, N, E^*)$, shell and pairing corrections, and to fit the value of the ratio $a_f/a_n$ for obtaining a good description of the energy dependence of nuclear fissility $P_f$. But it is impossible to describe well experimental $P_f$ simultaneously for all nuclides with a fixed set of these options. The theoretical $P_f$ is most sensitive to the value of $a_f/a_n$ used in calculation, and for different targets we have to use different values for this ratio to describe well the data. This problem is well known in literature and several systematics for the dependence of the value $a_f/a_n$ on nuclei targets have been proposed (see, e.g., Refs.[35, 36]).

The CEM is able to describe satisfactorily also the absolute value of photofission cross sections, but the agreement with the experimental data is not so good as for fissilities, due to an underestimation of the experimental total photoabsorption cross sections at photon energies $E_\gamma \simeq 400 - 600$ MeV (see, e.g., Fig. 1). As an example, the incident photon energy dependence of the calculated fission cross section for $^{238}$U is compared in Fig. 5 with the recent data[37]. For comparison, calculated total photoabsorption cross section is shown in figure by a long-dashed line, too. One can see that by choosing the corresponding value for the ratio $a_f/a_n$ the CEM reproduces with an accuracy of $\sim 30\%$ the shape and absolute value of the experimental fission cross section, independently of the form of the dependence $B_f(E^*)$ used in calculations. The underestimation of the data in the region

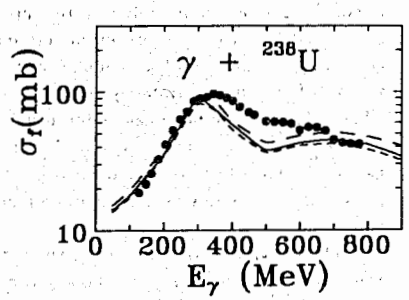


**Fig. 5.** The photofission cross section for $^{238}$U. The experimental points are from Ref.[37]. Calculations were performed with $a_f/a_n$ = 1.05, fission barriers $B_f$ from Ref.[38], shell and pairing corrections from Ref.[39], third systematics for $a(Z, N, E^*)$ from Ref[36], for the dependence of $B_f$ on excitation energy $E^*$ proposed in Ref.[40] (full line), as well as without a dependence of $B_f$ on $E^*$ (short-dashed line). The long-dashed line shows the total photoabsorption cross section predicted by the CEM.



$E_\gamma \simeq 400 - 600$ MeV is related with a small underestimation of the total photoabsorption cross section in this region.

As it was mentioned in the introduction, mechanisms of fast backward particle production in the cumulative (i.e., kinematically forbidden for quasi-free intranuclear projectile-nucleon collisions) region were intensively discussed at previous Dubna International Seminars on High Energy Physics Problems. More than fifty rather different models have been proposed to interpret cumulative particle production (see, e.g., [21] and references therein). Note should be made that the majority of these models has been proposed specifically to interpret cumulative particle production by means of special mechanisms. They consider only single-particle scattering processes and neglect the effects of rescattering and final state interaction, nevertheless, they succeeded in fitting shapes of experimental particle spectra.

It is of interest to estimate the contribution of "background" or conventional nuclear mechanisms in the framework of models that are not specially proposed for the description of cumulative particle production. Such models are our CEM and ORNL ICM. Let us show here, as an example, one our result related with this problem. Fig. 6 shows a comparison of predicted inclusive proton spectra by the CEM with $^{12}$C(γ,p)X data of Ref.[33], and with the direct knockout model[11], and a quasideuteron model[34].

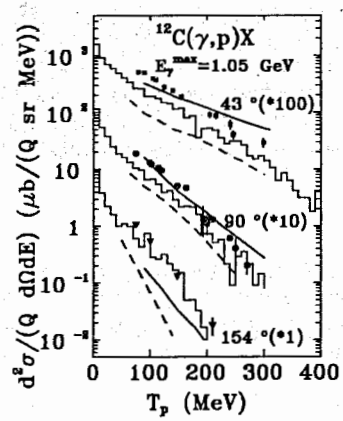


**Fig. 6.** Comparison of predicted inclusive photoproton spectra by the CEM (histograms are the sum of all three CEM components) with $^{12}$C(γ,p)X data of Ref.[33], and with the direct knockout[11] (solide lines), and a quasideuteron model[34] (dashed lines).

One can see that a good agreement with experimental data in both the shape and the absolute value has been obtained for protons emitted at both forward and backward angles. Apparently, as in the case of nucleon- and pion-induced reactions (see [21] and references therein), the "background" nuclear mechanisms also determine the main part of fast backward particle production at intermediate energies in reactions induced by photons.

**4.2. GDR Region.** We have analyzed a variety of photon absorption, elastic and inelastic cross sections for different nuclei in the energy region of the GDR using a group theory formalism[17] based on the interacting boson model (IBM)[18, 19]. Low-energy collective modes in nuclei can be described within the framework of the IBM model[18] by means of suitable boson degrees of freedom which approximate coherent pairs of neutrons and protons in the valence shells, coupled to angular momenta and parities $0^+$ and $2^+$ (s and d bosons, respectively). This algebraic approach has been proved to be a simple yet accurate tool to deal with spectroscopic properties of medium- and heavy-mass nuclei above all in share-transitional regions[18], where shell model calculations are not feasible and the simple geometric approach does not apply. In particular, even for a few valence nucleons, the number of states of a given angular momentum can be as high as $10^6 - 10^{12}$ and the dimensions of the relevant calculations become prohibitive for the present computing facilities. This fact is magnified as far as the treatment of giant resonance is concerned, since excitations across major shell are involved. The interacting boson model can be easily extended to allow us the description of high-lying giant resonances by adding suitable

degrees of freedom to the sd boson space[19]. In particular, the isovector giant dipole resonance is described by means of a p boson representing a collective particle-hole $J^\pi = 1^-$ $1\hbar\omega$ excitation. Then, the full IBM Hamiltonian reads as

$$\overline{H} = \overline{H}_{sd} + \overline{H}_p + \overline{H}_{sd,p} \ , \tag{7}$$

where $\overline{H}_{sd}$ is the usual IBM Hamiltonian[18, 19], relevant to low-lying states, $\overline{H}_p$ is proportional to the unperturbed p-boson energy following the empirical giant-dipole energy behaviour, $\epsilon_p \simeq 73 \times A^{-1/3}$ MeV, and $\overline{H}_{sd,p}$ gives the coupling between the low-energy quadrupole (vibrational, rotational) excitations and the dipole resonance excitation. This last term is dominated by a quadrupole-quadrupole interaction[19, 17]. Once calculated the GDR states by diagonalizing Hamiltonian (7), whose typical dimension is of the order of 50-60, the electromagnetic excitation can be estimated making use of the following E1 transition operator:

$$\overline{T}(E1) = \alpha(p^+ + p) \ , \tag{8}$$

with $\alpha$ adjustable parameter. The absorption and scattering cross sections of photons in the GDR region can be then obtained from the usual nuclear polarizabilities, assuming a suitable power-law dependence for the decay width[17] associated with each GDR component. As an example of application of the IBM model, Fig. 7 shows a calculated photoabsorption cross section with measured one[41]. $^{100}$Mo has 58 neutrons and 42 protons corresponding to 4 neutron bosons and 4 (hole) proton bosons, respectively. The strength of the quadrupole-quadrupole interaction between s, d and p bosons is 0.25 MeV, while the $\alpha$ parameter in Eq.(8) is chosen to 7.9 e fm. One can see that our calculations are in quite good agreement with experimental data. Similar results have been obtained for other targets.

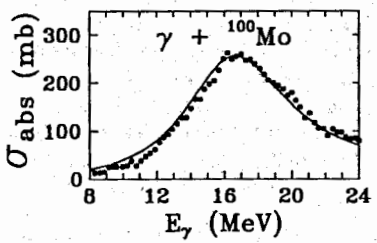


Fig. 7. Experimental[41] (dots) and calculated (line) photoabsorption cross section of $^{100}$Mo in the GDR region as a function of the photon energy.

## 5. Summary

So, we have shown that in the framework of our approach it is possible to describe in the absolute value the gross feature of a large variety of photonuclear reaction data for energies up to $\sim 1.2$ GeV, to analyze different mechanisms of absorption and interaction of photons with nuclei, and to estimate the relative role of different particle production mechanisms in these reactions.

Our results confirm the conclusion that the two-nucleon mechanism of photoabsorption is the main one in the quasideuteron region. The Monte Carlo method used in the CEM and ORNL ICM permits to calculate easily the contribution to every characteristics from each photodisintegration mode. But due to a large number of modes involved and to a little structure of data, it is difficult to extract much reliable information from analysis of inclusive characteristics. To clarify the question about the evidence of one-, three-, four-body, and other photodisintegration mechanisms and to estimate their relative role, data on



angular and energy distributions of different two correlated particle emission measured with monochromatic photons in a single experiment covering a wide energy and angular range are very useful. To our knowledge, by now, good measurements of such correlations have been performed only for low-mass nuclei like $^3$He[12] and $^6$Li[13]. Similar measurements for medium and heavy nuclei are desirable and possible at available at present high duty tagged photon beam facilities.

## References


[1] J. Ryckebusch et al., Nucl. Phys. **A568** (1994) 828.

[2] N. Bianchi et. al., Phys. Lett. **B325** (1994) 333.

[3] J.D.T. Arruda-Neto et al., Phys. Rev. **C48** (1993) 1594.

[4] R.C. Carrasco, M.J. Vicente Vacas and E. Oset, Nucl. Phys. **A570** (1994) 701.

[5] J.T. Londergan and G.D. Dixon, Phys. Rev. **C19** (1979) 998.

[6] M. Gari and H. Heback, Phys. Reports **72** (1981) 1.

[7] J. Arends et al., Z. Phys. **A298** (1980) 103.

[8] M. Kanazawa et al., Phys. Rev. **C35** (1987) 1828.

[9] D. Nilsson *et al.*, Physica Scripta **49** (1994) 397.

[10] G. van der Steenhoven and H.P. Blok, Phys. Rev. **C42** (1990) 2597.

[11] D.H. Boal and R.M. Woloshin, Phys. Rev. **C23** (1981) 1206.

[12] V. Isbert *et al.*, Nucl. Phys. **A578** (1994) 525;
T. Emura *et al.*, Phys. Rev. Lett. **73** (1994) 404; references given therein.

[13] D. Ryckbosch *et al.*, Nucl. Phys. **A568** (1994) 52 and references therein.

[14] R.C. Carrasco and E. Oset, Nucl. Phys. **A536** (1992) 445.

[15] K.K. Gudima, S.G. Mashnik and V.D. Toneev, Nucl. Phys. **A401** (1983) 329.

[16] T.A. Gabriel and R.G. Alsmiler, Phys. Rev. **182** (1969) 1035; T.A. Gabriel, Phys. Rev. **C13** (1976) 240.

[17] G. Maino, in *Dynamical Symmetries and Chaotic Behaviour in Physical Systems*, World Scientific, Singapore (1991), p.141, and references quatted therein.

[18] F. Iachello and A. Arima, *The Interacting Boson Model*, Cambridge University Press, Cambridge (1987).

[19] F. Iachello and P. Van Isacker, *The Interacting Boson-Fermion Model*, Cambridge University Press, Cambridge (1991).

[20] V.S. Barashenkov and V.D. Toneev, *Interaction of high energy particles and nuclei with atomic nuclei*, Atomizdat, Moscow (1972) in Russian.

[21] S.G. Mashnik, Nucl. Phys. **A568** (1994) 703.

[22] S. G. Mashnik, Revue Roum. Phys. **37** (1992) 179 and references therein.

[23] S.G. Mashnik, Acta Phys. Slov. **43** (1993) 243; ibid. **43** (1993) 86.

[24] M. Blann, H. Gruppelar, P. Nagel and J. Rodens, *International Code Comparison for Intermediate Energy Nuclear Data*, OECD, Paris (1994).

[25] K.K. Gudima, A.S. Iljinov and V.D. Toneev, Communication JINR P2-4661, Dubna (1969); V.S. Barashenkov, F.G. Geregi, A.S. Iljinov, G.G. Jonsson and V.D. Toneev, Nucl. Phys. **A231** (1974) 462.

[26] F.G. Gereghi, V.A. Zolotarevsky, K.K. Gudima, S.G. Mashnik and L.V. Bordianu, *Calculation of Photoneutron Reactions Cross Sections*, Report No. 01870081266, Kishinev State University, Kishinev (1990) in Russian

[27] J.S. Levinger, Phys. Rev. **84** (1951) 43.
[28] H.W. Bertini, Phys. Rev. **131** (1963) 1801.
[29] L. Dresner, Oak Ridge National Laboratori Report No. ORNL-CF-61-12-30 (1961).
[30] J. Arends *et al.*, Phys. Lett. **B98** (1981) 423.
[31] E.A. Arakelyan *et al.*, Sov. J. Nucl. Phys. **38** (1983) 589.
[32] P. Dougan and W. Stiefler, Z. Phys. **265** (1973) 1
[33] D.N. Olson, Ph.D. thesis, Cornell University, 1960.
[34] J.L. Mattews and W. Turchinetz, LNS Internal Report No. 110., 1966.
[35] J.B. Martins *et al.*, Phys. Rev. **C44** (1991) 354,
O.A.P. Tavares *et al.*, J. Phys. G: Nucl. Part. Phys. **19** (1993) 2145.
[36] A.S. Iljinov, M.V. Mebel *et al.*, Nucl. Phys. **A543** (1992) 517.
[37] T. Frommhold *et al.*, Phys. Lett. **B295** (1992) 28.
[38] H.J. Krappe, J.R. Nix and A.J. Sierk, Phys. Rev. **C20** (1979) 992.
[39] A.G.W. Cameron, Can. J. Phys. **35** (1957) 1021.
[40] V.S. Barashenkov, F.G. Geregi, A.S. Iljinov and V.D. Toneev, Nucl. Phys. **A222** (1974) 204.
[41] H. Beil *et al.*, Nucl. Phys. **A227** (1974) 427.

Received by Publishing Department
on October 28, 1994.